On the orientation dependence of the pressure and frictional drag experienced by spheroids in creeping flow

R. Ouchene

On the orientation dependence of the pressure and frictional drag experienced by spheroids in creeping flow

R. Ouchene[1,2,a)]
[1)] *CNRS, Institut Pprime, UPR 3346, 11 Boulevard Marie et Pierre Curie, Site du futuroscope, 86073 Poitiers, France*
[2)] *CNRS, LEMTA, UMR 7563, Université de Lorraine, 2 rue Jean Lamour, 54500 Vandoeuvre-les-Nancy, France*

The present work deals with the creeping flow past a single oblate or prolate spheroid. On the basis of the investigations of Aoi [T Aoi, Journal of the Physical Society of Japan, 10, 119 (1955)] on the contributions of pressure and frictional drag to the total drag experienced by spheroids when the fluid streams with a speed parallel to the axis of symmetry, we find that the pressure contribution corresponds to half of the dimensionless shape factor γ_0 provided by Happel & Brenner [Happel & Brenner, Inc. Englewood Cliffs, NJ 331, 1965]. Accordingly, we conjecture the validity of this finding when the fluid streams with a speed perpendicular to the axis of symmetry. Therefore, the formulations of dimensionless shape factors $\alpha_0/2$ and $\beta_0/2$ are confronted to numerical results at particle Reynolds number of 0.1. Furthermore, formulations of the pressure and the frictional drag are deduced and extended to any orientation relative to the flow direction. These results give physical insight into the total drag experienced by spheroids in creeping flow and can be helpful for the validation of simulations of the flow past an obstacle.

Keywords: Pressure drag, frictional drag, spheroid.

I. INTRODUCTION

Non-spherical particles are encountered in many environmental and industrial applications : pollen transport microorganisms[1], sediment transport in estuaries[2], ice crystals in the atmosphere[3,4], planktonic and swimming microorganisms[5–8], pulp and paper[9], or pulverized solid fuels[10–12], pneumatic conveying of granular materials[13].

The resistance to flow of solid non-spherical particle in viscous fluid has been more and more investigated in the last 50 years. In the past few decades, numerous numerical investigations has been largely focused on the drag force acting on non-spherical particles, especially spheroids which allow studying of shapes ranging from slightly deformed spheres to flatten spheroids (disks) and elongated spheroids (needles). Most of these studies, have been dedicated to provide physical insight on the flow around spheroids over the Stoksian assumption, i.e., a particle Reynolds number greater than unity. Moreover, many semi-empirical formulations have been provided to estimate the drag coefficient for a finite and moderate Reynolds number[14–30]. The pertinent literature on the hydrodynamic forces acting on spheroidal particles has been thoroughly reviewed in our previous work[31–34]; therefore, keeping in view the scope of the present work and for the sake of brevity and clarity, this actual review is restricted to the investigation of the pressure drag and frictional drag acting on spheroid in creeping flow.

The creeping motion past spheroid, i.e., when inertial effects are negligible in comparison with those of viscosity ($Re \ll 1$), has been originally investigated by Oberbeck[35]. The author solved the Stokes flow problem for a spheroid immersed in a uniform flow, and also treated the special cases of a circular disk. Ray[36] provided the solution to this circular disk problem in a different form and yields the same drag as Oberbeck formula. By making use of an exact solution of Oseen's equation of motion, Aoi[37] discussed theoretically the motion of the steady flow of an incompressible viscous flow past oblate or prolate spheroids when the axis of symmetry is aligned with the flow direction. The analytical exact solution of Oseen's equation is given in addition to the contribution of pressure and frictional drag experienced by spheroids. The hydrodynamic drag force acting on a spheroidal particle in a general flow field under the Stoksian assumption was obtained By Happel & Brenner[38]. Payne et al.[39] consider the solution of the Stokes flow problem for axially symmetric bodies (including spheroids) using the generalized axially symmetric potential theory initiated and developed by Weinstein[40,41] and obtain a general expression for the drag of a variety of axially symmetric bluff bodies.

According to Tomotika & Aoi[42] and Clift et al.[43], two thirds of the total drag arises from skin friction and a third from "form drag" in the case of a spherical particle. Both pressure drag and frictional drag contribute to the total drag force of spheroids and their relative importance is a function of spheroid elongation or flattening. Notwithstanding the importance of understanding the contributions of the pressure drag and frictional drag to the total drag, from a physical point of view and for the validation of the computational fluid dynamics codes, there is a lack of information about these contributions. Investigation of the contribution of pressure and frictional drag on the total drag experienced by spheroids perhaps has been first performed by Aoi[37]. Under the Stoksian assumption $Re_p \ll 1$, the author noticed that the ratio of the pressure to frictional drag

a)Electronic mail: r.ouchene1@gmail.com

is independent of the particle Reynolds number. Decomposing the total drag into form and frictional drag, Leith[44] expressed the total drag through the diameters of spheres with equal projected and effective surface areas, rather than through the dimensions of the object directly. Masliyah & Epstein[14] compared the results of simulations with Aoi's expressions of pressure and frictional drag and found a good agreement, even at $Re_p = 1$. Their computational results show that friction drag tends to vanish as the aspect ratio approaches zero and increases in significance for the larger aspect ratio. When the particle Reynolds number is greater than unity, Clift et al[43] found that the relative significance of frictional drag exhibits a substancial dependance on the particle Reynolds number. Moreover, Masliyah & Epstein[14] and Pitter et al.[15] revealed that, whatever the value of aspect ratio, the relative significance of frictional drag decreases with increasing particle Reynolds number. Holzer & Sommerfeld used a similar approach as Leith for quantifying the pressure and frictional drag. The authors used the sphericity (the ratio between the surface area of the volume equivalent sphere and the surface area of the considered particle) and the crosswise sphericity (the ratio between the cross-sectional area of the volume equivalent sphere and the projected cross-sectional area of the considered particle perpendicular to the flow). By compiling data available in the literature, the authors provided a new correlation for the total drag acting on non-spherical particle. Kishore & Gu[24] performed a numerical simulation of the flow past spheroid and noticed that the pressure, the frictional and the total drag coefficients of prolate spheroidal particles are larger than those of solid spheres and opposite trends have been observed for the oblate spheroidal particles. Particle-resolved simulation which fully considers the temperature-dependence of fluid properties has been performed by Fu et al.[45] with the purpose of studying the momentum and heat transfer between a high-temperature ellipsoidal particle and the fluid. The authors noticed that the increases of the drag force is mainly due to the pressure difference between the lower and upper surfaces of the particle at small angle of incidence, while the friction drag plays a dominant role in the increase of drag at higher incidence angle.

Unfortunately, in those investigations recounted here before, the focus has only been on the fluid streaming with a speed parallel to the axis of symmetry. Ouchene et al.[31] examined the contribution of the pressure and frictional drag on the total drag for the prolate spheroids. The authors noted that the pressure and the frictional contributions to the total drag force vary with the particle Reynolds number, aspect ratio, and angle of incidence and the frictional drag part is the main contribution to the total drag. Recently, Lain et al.[46] investigated by numerical the influence of simple shear flow on resistance coefficients. The authors find that the pressure and frictional drag coefficients are independent of the shear flow. However, there may exist an apparent difference in shear flow cases, where the flow speed is perpendicular to the axis of symmetry because the non-uniform effect of shear flow may rotate the particle.

As far as we are aware, the contribution of pressure and frictional drag experienced by spheroids has been only revealed when the axis of symmetry is aligned with the flow stream direction. This is attributed to the fact that fluid motion perpendicular to the axis of symmetry cannot be treated by the methods for axisymmetric motion. Therefore, we examine in this paper the pressure and frictional drag in this case of special interest corresponding to the fluid motion perpendicular to the axis of symmetry. Accordingly, the influence of the orientation is analysed.

II. THEORETICAL ANALYSIS

As it is well-known[47], in the steady incompressible creeping flow past a spheroid and under the Stoksian assumption, hydrodynamic drag force $\mathbf{F_D}$ acting on a spheroid can be expressed in the particle frame as:

$$\mathbf{F_D} = \mu \mathbf{K}(\mathbf{u_f} - \mathbf{u_p}) \tag{1}$$

where μ represents the dynamic viscosity of the fluid and $(\mathbf{u_f} - \mathbf{u_p})$ represents the relative velocity between the fluid velocity at the particle location $\mathbf{u_f}$ and the particle velocity $\mathbf{u_p}$. The resistance tensor $\mathbf{K}$ in the particle frame (x,y,z) is a diagonal matrix in its principal axes. The components of this resistance tensor are also called "dynamic shape factors"[44]. The solution can be retrieved following the method by Oberbeck[35]. In this method, the velocity field for the flow around an ellipsoid with an axis x parallel to the stream velocity, U, and no-slip conditions on the ellipsoid surface was represented by Oberbeck by :

$$\begin{cases} u = A\frac{\partial^2 \Omega}{\partial x^2} + B\left(x\frac{\partial \chi}{x} - \chi\right) + U \\ v = A\frac{\partial^2 \Omega}{\partial x \partial y} + Bx\frac{\partial \chi}{\partial y} \\ w = A\frac{\partial^2 \Omega}{\partial x \partial z} + Bx\frac{\partial \chi}{\partial z} \end{cases} \tag{2}$$

where (u, v, w) are the components of the velocity vectors. Ω the gravitational potential for a solid homogeneous ellipsoid and χ the velocity potential. The values of A and B can be retrieved by making $u = v = w = 0$ at the surface of the ellipsoid. For once the resistance along a principal axis, by superposition, the general case of the ellipsoid with any orientation relative to the stream can be treated. More detailed and comprehensive solution can be retrieved in Happel & Brenner. According to Oberbeck[35], the solution to this system of equations lead to obtain the resistance tensor that can be expressed as :

$$\mathbf{K} = 16\pi abc\left[\frac{\mathbf{ii}}{\chi_0 - a^2\alpha_0} + \frac{\mathbf{jj}}{\chi_0 - b^2\beta_0} + \frac{\mathbf{kk}}{\chi_0 - c^2\gamma_0}\right] \tag{3}$$

where the dimensionless shape parameters α_0, β_0, γ_0, and χ_0 are given by Brenner[47] by the following integrals:

$$\chi_0 = abc \int_0^\infty \frac{d\lambda}{\Delta}$$

$$\alpha_0 = abc \int_0^\infty \frac{d\lambda}{(a^2+\lambda)\,\Delta}$$

$$\beta_0 = abc \int_0^\infty \frac{d\lambda}{(b^2+\lambda)\,\Delta}$$

$$\gamma_0 = abc \int_0^\infty \frac{d\lambda}{(c^2+\lambda)\,\Delta}$$

$$\Delta = \sqrt{(a^2+\lambda)\,(b^2+\lambda)\,(c^2+\lambda)}$$

Here a, b, and c are the semi-axis of the spheroid and λ is a dummy variable. $\mathbf{i}$, $\mathbf{j}$ and $\mathbf{k}$ are unit vectors in spheroid's system of coordinates. The different types of spheroids are illustrated in Figure I . Schematic configuration of the uniform inflow, the semi-axis (a, b and c) and incidence angle, ϕ are depicted in Figure II. It is worth mentioning that the semi-axis of symmetry a is always aligned with the x of the particle frame.

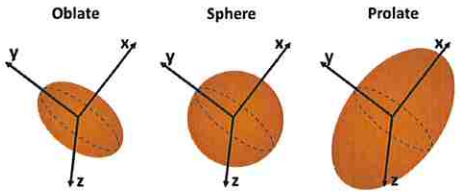

Figure 1. Illustration of the different types of Spheroids of revolution from oblate to prolate.

In table I, we reported the analytical expressions of the dimensionless shape factors α_0, β_0 and γ_0 for an axisymmetric spheroidal particle derived by Gallily & Cohen[48] and Siewert et al.[49].

The derivation of the drag force on a sphere in creeping flow ($Re_p \ll 1$) shows that two thirds of the total drag arises from "skin friction", i.e., the shear stress acting at the sphere surface, and one third from "Form drag", i.e., that originates from the pressure gradient across the surface of the sphere[42][43]. However, in the case of spheroids (prolate or oblate), contributions of form drag and skin friction differs from that of the sphere and results in an even more complex behavior depending on the particle aspect ratio $\beta = a/b$ and particle orientation. Here a corresponds to the semi-axis of symmetry and $b = c$ corresponds to the semi-axis normal to the axis of symmetry.

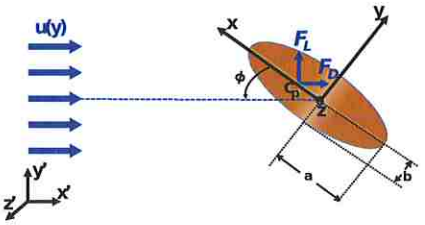

Figure 2. Schematic of the uniform inflow as well as the semi-axis (a, b and c) and incidence angle ϕ. The drag and lift forces are displayed at the center of pressure c_p.

$$\mathbf{F_D}(\beta) = \mathbf{F_{D,P}}(\beta) + \mathbf{F_{D,f}}(\beta) \tag{4}$$

where $\mathbf{F_{D,P}}$ and $\mathbf{F_{D,f}}$ are the pressure and frictianal drag forces.

By summing up the viscous stresses exerted by the fluid upon the surface of the body, and as far as the Oseen's approximation is concerned, Aoi[37] derived expressions for the contribution of the form drag to the total drag experienced by the spheroid when its axis of symmetry is aligned with the flow direction, $\delta_{p,\parallel} = ||\mathbf{F_{D,P,\parallel}}(\beta)||/||\mathbf{F_{D,\parallel}}(\beta)||$:

$$\delta_{p,\parallel} = (\tau_0^2+1)(1-\tau_0\cot^{-1}\tau_0) \quad for\ \beta < 1 \tag{5}$$

with $\tau_0 = \beta/\sqrt{1-\beta^2}$

$$\delta_{p,\parallel} = (t_0^2-1)\left[-1+\frac{t_0}{2}\ln\frac{t_0+1}{t_0-1}\right] \quad for\ \beta > 1 \tag{6}$$

with $t_0 = \beta/\sqrt{\beta^2-1}$.

The contribution of the frictional drag experienced by the spheroid $\delta_{f,\parallel} = ||\mathbf{F_{D,f,\parallel}}(\beta)||/||\mathbf{F_{D,\parallel}}(\beta)||$ is then given:

$$\delta_{f,\parallel} = 1 - \delta_{p,\parallel} \tag{7}$$

As stated by Aoi[37], these formulations show that the pressure drag and frictional drag experienced by spheroid contribute to the total drag in definite ratios which are independent of particle number Reynolds. It is readily recognized that, such approach can only be used when the fluid streams with a speed parallel to the axis of symmetry. To our knowledge, there are no available analytical results in the literature dealing with a fluid streaming with a speed normal to the axis of symmetry and/or different inclinations.

Table I. Dimensionless shape parameters α_0, β_0 and γ_0 for axisymetric spheroidal particle derived by Gallily & Cohen[48] and Siewert et al.[49].

	Oblate $\beta < 1$	Sphere	Prolate $\beta > 1$
χ_0	$\frac{a^2\beta}{\sqrt{1-\beta^2}}\left[\pi - 2\tan^{-1}\frac{\beta}{\sqrt{1-\beta^2}}\right]$	$2a^2$	$\frac{-a^2\beta}{\sqrt{\beta^2-1}}\ln\frac{\beta-\sqrt{\beta^2-1}}{\beta+\sqrt{\beta^2-1}}$
$\alpha_0 = \beta_0$	$-\frac{\beta}{2\sqrt{1-\beta^2}^3}\left[2\tan^{-1}\frac{\beta}{\sqrt{1-\beta^2}} - \pi + 2\beta\sqrt{1-\beta^2}\right]$	$\frac{2}{3}$	$\frac{\beta^2}{\beta^2-1}\frac{\beta}{2\sqrt{\beta^2-1}^3}\ln\frac{\beta-\sqrt{\beta^2-1}}{\beta+\sqrt{\beta^2-1}}$
γ_0	$\frac{1}{\sqrt{1-\beta^2}^3}\left[2\beta\tan^{-1}\frac{\beta}{\sqrt{1-\beta^2}} - \pi\beta + 2\sqrt{1-\beta^2}\right]$	$\frac{2}{3}$	$-\frac{2}{\beta^2-1} - \frac{\beta}{\sqrt{\beta^2-1}^3}\ln\frac{\beta-\sqrt{\beta^2-1}}{\beta+\sqrt{\beta^2-1}}$

III. METHODOLOGY

In the present work, numerical results issued from our previous investigations dealing with prolate spheroids[31,50] of the aspect ratios of $\beta = 1, 1.25, 2.5, 5, 10, 16$ and 32 combined with the investigations dealing with oblate spheroids the aspect ratios of $\beta = 0.2, 0.5, 0.8$, obtained for $Re_p = 0.1$ are used as cases of reference. Here, the particle Reynolds number is defined as $Re_p = \frac{|\mathbf{u_R}|d_p}{\nu}$, where $\mathbf{u_R} = \mathbf{u_f} - \mathbf{u_p}$ is the relative velocity between the particle $\mathbf{u_p}$ and the fluid $\mathbf{u_f}$, d_p is the diameter of the volume equivalent sphere and ν is the kinematic viscosity.

The numerical approach described in Ouchene et al.[31,50] is briefly recalled here to keep the paper self-contained.The numerical results have been obtained with a steady-state simulations using the CFD code Ansys Fluent. Centered scheme has been used for discretizing all the numerical fluxes in the Navier-Stokes equations. The problem of the coupling between velocity and pressure has been tackled with a Semi-Implicit Method for Pressure-Linked Equations (SIMPLE)[51]. In this body-fitted approach, the fluid volume has been discretized into unstructured tetrahedral control volumes while a triangular surface mesh has been used for the surface of the particle immersed in the fluid. The mesh surface of the particle is sufficiently fine to give an accurate integration of the forces acting on the particle surface. The mesh quality was analysed by testing three meshes for the prolate spheroids and the results were considered mesh independent for a number larger 650000. In the case of oblate spheroids similar test was conducted and the results found to be independent over 900000 cells. Because of the high number of nodes, the calculations were performed by Message Passing Interface parallel programming (eight processors). The central processing unit (CPU) time is of the order of 7 h for both oblate and prolate.

In order to provide expressions for the pressure drag and frictional drag experienced by the spheroid when the fluid streams with a speed normal to the axis of symmetry, the following approach is used:

- Compute the ratio of the pressure drag to the total resistance $\delta_{p,\perp} = ||\mathbf{F_{D,p},\perp}(\beta)||/||\mathbf{F_{D,\perp}}(\beta)||$.
- Provide the best functional form of $\delta_{p,\perp}$.
- Deduce the expression of δ_p as a function of the spheroid inclination with respect to the flow.
- The ratio of the frictional drag to the total resistance is allways obtained by $\delta_{f,\perp} = 1 - \delta_{p,\perp}$

Before the presentation of the new results and formulas, the accuracy of the numerical method is first assessed through a comparison of the numerical results with known test cases. It was shown in Ouchene et al.[31] that the simulations give very good results with respect to the well-known drag correlation of Schiller and Naumann for the case of spherical particle. A good accordance between the computed drag and lift coefficients results and the analytical solution given in Happel and Brenner[38] for both prolate and oblate spheroids in[33,34].

Here, we present an additional relevant validation test of the numerical technique. The computational results of the ratios of the pressure and frictional drag to the total resistance when the fluid streams parallel to the axis of symmetry $\delta_{p,||}$ and $\delta_{f,||}$ for the 10 aspect ratios are compared to the analytical formulas provided by Aoi[37] (Fig.3) at particle Reynolds number $Re_p = 0.1$.

Figure 3 shows clearly that the results of simulations are in good agreement with Aoi's formulas both qualitatively and quantitatively, regardless the aspect ratio. According to the different validation tests reported in our previous works as well as the present additional validation case, the results simulations of the flow around the oblate and prolate spheroidal particle issued from work[31,33,34,50] are relevant for the purpose of the present work.

IV. RESULTS AND DISCUSSION

Following the methodology described herein before, we compute and plot the ratio of the pressure and frictional drag to the total resistance, respectively $\delta_{p,\perp}$ and $\delta_{f,\perp}$, as a function of the aspect ratio at $Re_p = 0.1$.

It is seen that the contribution of the pressure to the total resistance,$\delta_{p,\perp}$, increases with increasing aspect ratio. This contribution tends to vanish in the case of a circular disc ($\beta \to 0$), achieves 1/3 in the case of a sphere and

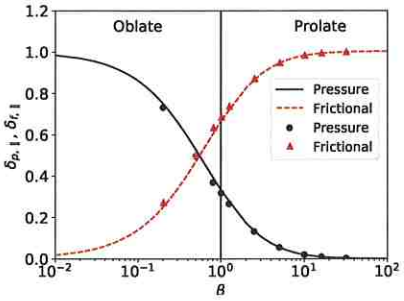

Figure 3. Ratio of the pressure and frictional drag to the total resistance($\delta_{p,\parallel}$ and $\delta_{f,\parallel}$) as a function of aspect ratio β. Lines correspond to the Aoi's formulas (Eqs. 5-6 and eqs.7) and symbols correspond to the numerical results

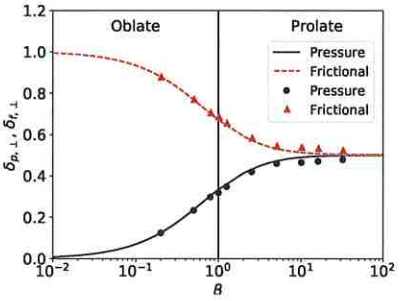

Figure 4. Ratio of the pressure and frictional drag to the total resistance($\delta_{p,\perp}$ and $\delta_{f,\perp}$) as a function of aspect ratio β. Lines correspond to the formulas (Eqs.10-11 and Eq.7) and symbols correspond to the numerical results

reaches an asymptotic value of 0.5 for the higher aspect ratio. An opposite behaviour can be seen for the contribution of the frictional to the total resistance $\delta_{f,\perp}$, i.e., it tends to unity in the case of a circular disc ($\beta \to 0$), achieves $2/3$ in the case of a sphere and reaches an asymptotic value of 0.5 for the higher aspect ratio.

To select the best functional form for the new formulas, we first paid specific attention to the analytical formulas provided by Aoi (Eqs. 5-6), when the fluid streams parallel to the axis of symmetry Eqs (5-6). By rewriting these expressions in the forms which are suitable for the analysis, we obtain after a little algebra for oblate spheroid:

$$\begin{aligned}\delta_{p,\parallel} &= (\tau_0^2+1)(1-\tau_0\cot^{-1}\tau_0)\\ &= \frac{1}{\sqrt{1-\beta^2}^3}\left[\beta\tan^{-1}\frac{\beta}{\sqrt{1-\beta^2}} - \frac{\pi}{2}\beta + \sqrt{1-\beta^2}\right]\\ &= \frac{a^3\beta}{2}\int_0^\infty \frac{d\lambda}{(c^2+\lambda)\,\Delta}\end{aligned} \tag{8}$$

Similarly, for prolate spheroid:

$$\begin{aligned}\delta_{p,\parallel} &= (t_0^2-1)\left[-1+\frac{t_0}{2}\ln\frac{t_0+1}{t_0-1}\right]\\ &= -\frac{1}{\beta^2-1} - \frac{\beta}{2\sqrt{\beta^2-1}^3}\ln\frac{\beta-\sqrt{\beta^2-1}}{\beta+\sqrt{\beta^2-1}}\\ &= \frac{a^3\beta}{2}\int_0^\infty \frac{d\lambda}{(c^2+\lambda)\,\Delta}\end{aligned} \tag{9}$$

With this new representation, an inspection of the expressions (Eqs. 8-9) lead to gaining further knowledge of the Aoi's formulas. Surprisingly, (Eqs.8-9) reveals that the ratio of the pressure drag to the total drag $\delta_{p,\parallel}$ corresponds to half of the dimensionless shape parameter γ_0 (See Table. I). This observation is crucial since it discloses a link between the Aoi's formulas and the dimensionless shape parameters which have been not reported until now. Furthermore, the capital interest consists of providing a physical meaning for the dimensionless shape parameter γ_0, which corresponds to twice the pressure drag contribution to the total drag $\delta_{p,\parallel}$.

We now turn our attention to the ratio of the pressure to the total resistance when the fluid streaming perpendicular to the axis of symmetry. One might be tempted to conclude that the above statement, i.e., $\delta_{p,\parallel} = \gamma_0/2$ when the fluid streams parallel to the axis of symmetry, holds for the fluid streaming perpendicular to the axis of symmetry, i.e., $\alpha_0 = \beta_0 = 2\delta_{p,\perp}$. Accordingly, instead of performing a fitting of the numerical results, the relevant functional forms of $\delta_{p,\perp}$ are tested in comparison with the numerical results.
For $\beta < 1$:

$$\delta_{p,\perp} = -\frac{\beta}{2\sqrt{1-\beta^2}^3}\left[\tan^{-1}\frac{\beta}{\sqrt{1-\beta^2}} - \frac{\pi}{2} + \beta\sqrt{1-\beta^2}\right], \tag{10}$$

and for $\beta > 1$:

$$\delta_{p,\perp} = \frac{1}{2}\left[\frac{\beta^2}{\beta^2-1} + \frac{\beta}{2\sqrt{\beta^2-1}^3}\ln\frac{\beta-\sqrt{\beta^2-1}}{\beta+\sqrt{\beta^2-1}}\right] \tag{11}$$

Figure 4, shows clearly that the above formulas reproduce both qualitatively and quantitatively the numerical results. The mean average relative deviation is 2.77% which rises to a maximum of 5.09%. This indicates that equations 10-11 predict very well the contribution of the pressure to the total resistance.

At this stage, the expressions for the pressure drag contribution to total drag force $\delta_{p,\perp}(\beta)$ have been drawn

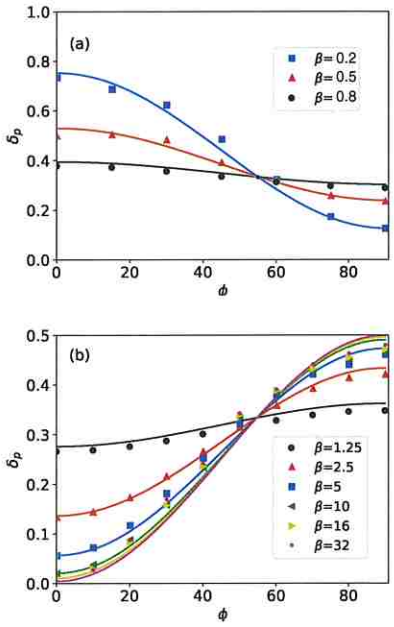

Figure 5. Ratio of the pressure drag to the total resistance (δ_p as a function of the incidence angle ϕ for oblate spheroids $\beta < 1$ (a) and for prolate ellipsoids $\beta > 1$ (b). Lines correspond to Eq.14, for the corresponding aspect ratio.

but the expression for $\delta_p(\beta, \phi)$ remains to be determined. For this purpose, we have to bear mind that the total resistance at any orientation with respect to the streaming flow, ϕ, can be written as:

$$\mathbf{F_D}(\beta, \phi) = \mathbf{F_{D,\parallel}}(\beta) + \left(\mathbf{F_{D,\perp}}(\beta) - \mathbf{F_{D,\parallel}}(\beta)\right) \sin^2 \phi \quad (12)$$

and

$$\mathbf{F_D}(\beta, \phi) = \mathbf{F_{D,p}}(\beta, \phi) + \mathbf{F_{D,f}}(\beta, \phi) \quad (13)$$

By combining these two equations (12-13) and by superposition we also obtain the dependence of pressure contribution $\delta_p(\beta, \phi)$ with particle orientation for both prolate and oblate spheroids reads as:

$$\delta_p(\beta, \phi) = \delta_{p,\parallel}(\beta) + (\delta_{p,\perp}(\beta) - \delta_{p,\parallel}(\beta)) \sin^2 \phi \quad (14)$$

This quantity is plotted in figure 5 for the different aspect ratios considered in the present study. It can be seen that the pressure contribution decreases with the increasing of incidence angle ϕ for oblate spheroids and increases with respect to the incidence angle for the prolate spheroids. It is evident that this behaviour arises from the difference of the surface areas facing the flow. Indeed, the surface area facing the flow is larger when the revolution axis of the oblate is parallel with the flow direction. In opposite, the surface area facing the flow is smaller when the revolution axis of the prolate is parallel with the flow direction. Compared to the results of simulations given by ouchene et al.[31,50] , equation 14 gives a good estimation of the pressure drag contribution to the total drag, whatever the aspect ratio and incidence angle.

Further, it is interesting to notice the existence of angle $\phi^*_{oblate} = \phi^*_{prolate} \approx 55.8^o$ at which the pressure contribution remains the same whatever the particle aspect ratio.

V. CONCLUSION

The pertinent literature on the hydrodynamic forces acting on spheroidal particles shows that the contribution of pressure and frictional drag experienced by spheroids has been only revealed when the axis of symmetry is aligned with the flow stream direction. From the analysis of the expressions provided by Aoi[37], we reveal that the pressure contribution corresponds to the half of the dimensionless shape factor γ_0 reported by Happel & Brenner[38], when the fluid streams parallel to the axis of symmetry.

Did this finding applicable when the fluid streams perpendicular to the axis of symmetry? The comparison with the numerical results indicates that the contribution of the pressure drag corresponds to the half of the dimensionless shape factors α_0 and β_0. Note that the present finding is only valid in the range of aspect ratio investigated in this study. However, we conjecture that the finding remains valid whatever the aspect ratio. This can a subject of future studies.

By making use of the above finding, we provide an expression of the pressure contribution $\delta_p(\beta, \phi)$ as a function of particle aspect ratio and particle orientation with respect to the flow direction. This allows us to notice the existence of an angle $\phi^* \approx 55.8^o$ for which the pressure contribution remains constant regardless the particle aspect ratio.

These results give physical insight into the total drag experienced by spheroids in creeping flow and can be helpful for the validation of simulations of the flow past an obstacle.

It should be highlighted that the present contribution is achieved for a small particle Reynolds number, thereby the formulas have to be used carefully. An interesting issue for the future investigation is studying the contributions of the pressure and viscous drag with respect to particle Reynolds number and attempt to provide formulas for those contributions.

REFERENCES

[1]D. Mourelle and A. R. Prieto, "Pollen and spores from surface samples in the campos region of uruguay and their paleoecological implications," Acta Botanica Brasilica **30**, 351–370 (2016).

[2]A. J. Mehta, *An introduction to hydraulics of fine sediment transport*, Vol. 38 (World Scientific Publishing Company, 2013).

[3]R. A. Shaw, "Particle-turbulence interactions in atmospheric clouds," Annual Review of Fluid Mechanics **35**, 183–227 (2003).

[4]A. Korolev and G. Isaac, "Roundness and aspect ratio of particles in ice clouds," Journal of the atmospheric sciences **60**, 1795–1808 (2003).

[5]J. S. Guasto, R. Rusconi, and R. Stocker, "Fluid mechanics of planktonic microorganisms," Annual Review of Fluid Mechanics **44**, 373–400 (2012).

[6]T. Pedley and J. O. Kessler, "Hydrodynamic phenomena in suspensions of swimming microorganisms," Annual Review of Fluid Mechanics **24**, 313–358 (1992).

[7]W. M. Durham, E. Climent, M. Barry, F. De Lillo, G. Boffetta, M. Cencini, and R. Stocker, "Turbulence drives microscale patches of motile phytoplankton," Nature communications **4**, 1–7 (2013).

[8]S. Lovecchio, E. Climent, R. Stocker, and W. M. Durham, "Chain formation can enhance the vertical migration of phytoplankton through turbulence," Science advances **5**, eaaw7879 (2019).

[9]F. Lundell, L. Söderberg, Daniel, and P. H. Alfredsson, "Fluid mechanics of papermaking," Annual Review of Fluid Mechanics **43**, 195–217 (2011).

[10]M. Mandø, "Turbulence modulation by non-spherical particles," (2009).

[11]J. Brix, P. A. Jensen, and A. D. Jensen, "Modeling char conversion under suspension fired conditions in o2/n2 and o2/co2 atmospheres," Fuel **90**, 2224–2239 (2011).

[12]M. C. Powers, "A new roundness scale for sedimentary particles," Journal of Sedimentary Research **23**, 117–119 (1953).

[13]L. Y. Lee, T. Y. Quek, R. Deng, M. B. Ray, and C.-H. Wang, "Pneumatic transport of granular materials through a 90 bend," Chemical Engineering Science **59**, 4637–4651 (2004).

[14]J. H. Masliyah and N. Epstein, "Numerical study of steady flow past spheroids," Journal of Fluid Mechanics **44**, 493–512 (1970).

[15]R. L.Pitter, H. R. Pruppacher, and A. E. Hamielec, "A numerical study of viscous flow past a thin oblate spheroid at low and intermediate reynolds numbers," Journal of the Atmospheric Sciences **30**, 125–134 (1973).

[16]J. Militzer, J. M. Kan, F. Hamdullahpur, P. R. Amyotte, and A. A. Taweel, "Drag coefficient for axisymmetric flow around individual spheroidal particles," Powder technology **57**, 193–195 (1989).

[17]A. Tripathi, R. P. Chhabra, and T. Sundararajan, "Power law fluid flow over spheroidal particles," Industrial & engineering chemistry research **33**, 403–410 (1994).

[18]J. Comer and C. Kleinstreuer, "A numerical investigation of laminar flow past nonspherical solids and droplets," J. Fluid Eng.Trans.ASME **117**, 170–175 (1995).

[19]B. J. O'Donnell and B. Helenbrook, "Drag on ellipsoids at finite reynolds numbers," Atomization and Sprays **15** (2005).

[20]A. Richter and P. A. Nikrityuk, "Drag forces and heat transfer coefficients for spherical, cuboidal and ellipsoidal particles in cross flow at sub-critical reynolds numbers," International Journal of Heat and Mass Transfer **55**, 1343–1354 (2012).

[21]M. Zastawny, G. Mallouppas, F. Zhao, and B. V. Wachem, "Derivation of drag and lift force and torque coefficients for nonspherical particles in flows," International Journal of Multiphase Flow **39**, 227–239 (2012).

[22]A. Richter and P. A. Nikrityuk, "New correlations for heat and fluid flow past ellipsoidal and cubic particles at different angles of attack," Powder technology **249**, 463–474 (2013).

[23]B. Arcen, R. Ouchene, M. Khalij, and A. Tanière, "Prolate spheroidal particles' behavior in a vertical wall-bounded turbulent flow," Physics of Fluids **29**, 093301 (2017).

[24]N. Kishore and S. Gu, "Momentum and heat transfer phenomena of spheroid particles at moderate reynolds and prandtl numbers," International Journal of Heat and Mass Transfer **54**, 2595–2601 (2011).

[25]S. K. Sanjeevi and J. T. Padding, "On the orientational dependence of drag experienced by spheroids," Journal of Fluid Mechanics **820**, R1 (2017).

[26]S. K. Sanjeevi, J. Kuipers, and J. T. Padding, "Drag, lift and torque correlations for non-spherical particles from stokes limit to high reynolds numbers," International Journal of Multiphase Flow **106**, 325–337 (2018).

[27]C. Ke, S. Shu, H. Zhang, H. Yuan, and D. Yang, "On the drag coefficient and averaged nusselt number of an ellipsoidal particle in a fluid," Powder Technology **325**, 134–144 (2018).

[28]Y. Cui, J. Ravnik, M. Hriberšek, and P. Steinmann, "A novel model for the lift force acting on a prolate spheroidal particle in an arbitrary non-uniform flow. part i. lift force due to the streamwise flow shear," International Journal of Multiphase Flow **104**, 103–112 (2018).

[29]Y. Cui, J. Ravnik, O. Verhnjak, M. Hriberšek, and P. Steinmann, "A novel model for the lift force acting on a prolate spheroidal particle in arbitrary non-uniform flow. part ii. lift force taking into account the non-streamwise flow shear," International Journal of Multiphase Flow **111**, 232–240 (2019).

[30]H. I. Andersson and F. Jiang, "Forces and torques on a prolate spheroid: Low-reynolds-number and attack angle effects," Acta Mechanica **230**, 431–447 (2019).

[31]R. Ouchene, M. Khalij, A. Tanière, and B. Arcen, "Drag, lift and torque coefficients for ellipsoidal particles: From low to moderate particle reynolds numbers," Computers & Fluids **113**, 53–64 (2015).

[32]R. Ouchene, A. Chadil, P. Fede, M. Khalij, A. Tanière, S. Vincent, J. L. Estivalezes, and B. Arcen, "Numerical simulation and modelling of the forces acting on single and multiple non-spherical particles," in *ASME 2014 4th Joint US-European Fluids Engineering Division Summer Meeting collocated with the ASME 2014 12th International Conference on Nanochannels, Microchannels, and Minichannels* (American Society of Mechanical Engineers, 2014) pp. V002T34A001–V002T34A001.

[33]R. Ouchene, M. Khalij, B. Arcen, and A.Tanière, "A new set of correlations of drag, lift and torque coefficients for non-spherical particles and large reynolds numbers," Powder Technology **303**, 33–43 (2016).

[34]R. Ouchene, "Numerical simulation and modeling of the hydrodynamic forces and torque acting on individual oblate spheroids," Physics of Fluids **32**, 073303 (2020).

[35]A. oberbeck1876, "uber stationare flussigkeitsbewegungen mit berucksichtigung der inner reibung," J. reine angew. Math , 62–80 (1876).

[36]M. Ray, "Xlvi. application of bessel functions to the solution of problem of motion of a circular disk in viscous liquid," The London, Edinburgh, and Dublin Philosophical Magazine and Journal of Science **21**, 546–564 (1936).

[37]T. Aoi, "The steady flow of viscous fluid past a fixed spheroidal obstacle at small reynolds numbers," Journal of the Physical Society of Japan **10**, 119–129 (1955).

[38]J. Happel and H. Brenner, "Low reynolds number hydrodynamics prentice-hall," Inc., Englewood Cliffs, NJ **331** (1965).

[39]L. E. Payne and W. H. Pell, "The stokes flow problem for a class of axially symmetric bodies," Journal of Fluid Mechanics **7**, 529–549 (1960).

[40]A. Weinstein, "Discontinuous integrals and generalized potential theory," Transactions of the American mathematical society **63**, 342–354 (1948).

[41]A. Weinstein, "On a class of partial differential equations of even order," Annali di Matematica Pura ed Applicata **39**, 245–254 (1955).

[42]S. Tomotika and T. Aoi, "The steady flow of viscous fluid past a sphere and circular cylinder at small reynolds numbers," The

Quarterly Journal of Mechanics and Applied Mathematics **3**, 141–161 (1950).
[43]R. Clift, J. Grace, and M. Weber, "Bubbles, drops and particles, acad," Press, New York , 117–120 (1978).
[44]D. Leith, "Drag on nonspherical objects," Aerosol science and technology **6**, 153–161 (1987).
[45]J. Fu, K. Jiang, S. Chen, and X. Du, "Effect of large temperature difference on drag coefficient and nusselt number of an ellipsoidal particle in compressible viscous flow," Powder Technology **408**, 117766 (2022).
[46]S. Laín, C. Castang, and M. Sommerfeld, "Study of flow resistance coefficients acting on regular non-spherical particles in simple shear flow at moderate reynolds numbers," Powder Technology **435**, 119428 (2024).
[47]H. Brenner, "The stokes resistance of an arbitrary particle—ii: An extension," Chemical Engineering Science **19**, 599–629 (1964).
[48]I. Gallily and A.-H. Cohen, "On the orderly nature of the motion of nonspherical aerosol particles. ii. inertial collision between a spherical large droplet and an axially symmetrical elongated particle," Journal of Colloid and Interface Science **68**, 338–356 (1979).
[49]C. Siewert, R. Kunnen, M. Meinke, and W. Schröder, "Orientation statistics and settling velocity of ellipsoids in decaying turbulence," Atmospheric research **142**, 45–56 (2014).
[50]R. Ouchene, *Dispersion de particules non-sphériques en écoulement turbulent*, Ph.D. thesis, Université de Lorraine (2015).
[51]S. V. Patankar and D. B. Spalding, "Mathematical-models of fluid-flow and heat-transfer in furnaces-review," Journal of the Institute of Fuel **46**, 279–283 (1973).

VI. ACKNOWLEDGMENTS

This work received funding by Pprime Laboratory; their support is gratefully acknowledged. Results of simulation are extracted from ANR-PLAYER(ANR-11-BS09-0004) and LEMTA laboratory; their support and help is acknowledged.